

# Quartz fluorescence backgrounds in rare-event searches

P. Sorensen<sup>1,\*</sup> and R. Gibbons<sup>1,2</sup>

<sup>1</sup>*Lawrence Berkeley National Laboratory, 1 Cyclotron Rd, Berkeley, CA 94720, USA*

<sup>2</sup>*University of California, Berkeley, Department of Physics, Berkeley, CA 94720, USA*

(Dated: June 11, 2025)

It has been known for almost a decade that delayed photon noise with a power law time profile follows scintillation pulses in liquid xenon particle detectors. The origin of the noise has remained unknown, and in the past two years, has become an overwhelming background for low-threshold dark matter searches aimed at  $\mathcal{O}(10)$  GeV dark matter particle masses, as well as measurements of coherent neutrino-nucleus scattering of  ${}^8\text{B}$  solar neutrinos. We show that the dominant component of this delayed photon noise is due to UV-induced fluorescence of quartz photosensor windows.

Astrophysical observations and cosmological data indicate the existence of non-luminous, non-baryonic massive dark matter [1, 2]. A favored candidate for this dark matter has been a hypothetical class of beyond-the-Standard-Model particles called Weakly Interacting Massive Particles (WIMPs) with typical masses in the range of 100 GeV/c<sup>2</sup> [3]. The most sensitive experiments searching for these particles use liquid xenon as a scattering target [4–6], deployed in a Time Projection Chamber (TPC) [7].

Particle interaction events in this class of TPC consist of a primary scintillation pulse of UV photons (S1), followed by electron drift, electron emission into the vapor, and an electron-induced proportional electroluminescence pulse of UV photons (S2). The S2 signal occurs anywhere up to about a millisecond later, depending on the distance the electrons drift. The amplitude of a typical S2 pulse is a detector-dependent  $\bar{a} \sim 10^5$  photons for a 1 MeV electron interaction. The dominant scintillation decay time is  $\tau = 27$  ns [8], and S1 pulses of interest can be as small as two single photons in a few hundred ns coincidence window.

In such detectors, it is known that ionizing events due to particle interactions are followed by a trickle of single electron signals extending in time for tens to hundreds of milliseconds after the originating event [9]. This delayed electron noise presents a fatal background for sub-GeV-mass dark matter searches in this class of detector [10]. Delayed electron noise was later found to be accompanied by delayed photon noise [11], both of which exhibit power law decay [12]. The delayed photon noise has been hypothesized to originate from PTFE fluorescence [11, 12]. We refer to the delayed photon noise as  $d_p(t) = \alpha \bar{a} t^k$  with  $\alpha$  generally proportional to the originating 175 nm UV photon pulse(s)  $\bar{a}$ . An investigation of  $d_p(t)$  in LZ found  $k = -1.3$  [13].

Accidental coincidence (often referred to as AC) backgrounds – partially caused by pile-up of the delayed photon noise – have recently become dominant in searches for low-mass dark matter candidates [14–16] and observation of  ${}^8\text{B}$  solar neutrinos [17, 18]. This is a reflection of the ultra-low radiogenic backgrounds these experiments have achieved. It is also somewhat striking, because in

the planning phases of these experiments, accidental coincidence backgrounds were either not mentioned [19], or were dismissed as sub-dominant [20].

The problem is exemplified in Fig. 1, showing simulated random  $\mathcal{O}(1)$  MeV background events (triangles) followed by a 40 ms trigger hold off. For each event, the (S1+S2) photon pulse occurs in a typical time  $< 1$  ms. The normalization of the post-event power law delayed photon noise (blue curves) was chosen to roughly agree with observations from LZ [21] (see e.g. Fig. 5.19 of [13]). The scale of the problem in XENONnT and PandaX-4T is expected to be similar, since they also use Hamamatsu R11410 photosensors. The exponential delayed photon noise (green dotted) is based on the present work. The base dark count rate  $R = 10$  kHz would be expected from 40 Hz per PMT [22] in a 250 PMT detector.

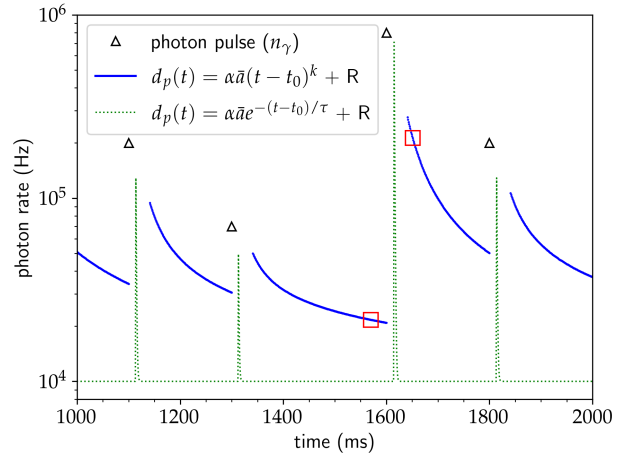


FIG. 1. Simulated background events (triangles) in a liquid xenon TPC dark matter search detector. The power law delayed photon rate (blue curve) is calculated from Eq. 5.6 of [13] with  $k = -1.3$ . The notional exponential delayed photon rate (green dotted curves) is based on the present work, assuming a base dark count rate  $R = 10$  kHz. Red squares indicate regions with a factor  $\times 1000$  difference in S1 AC.

The power law delayed photon noise perturbs the quiescent time between background events, during which the

experiments wish to look for small, rare signals with pulse sizes of  $\sim 0.5 \times 10^4$  photons or smaller. The regions indicated by the red squares have a factor  $\times 10$  difference in photon background rate. This increases the S1  $n = 3$  AC probability in a 200 ns window from 0.38 Hz to 380 Hz, as calculated from Eq. 4.1 of [23]. Rates for S1  $n = 2$  AC backgrounds are a factor  $\times 250$  higher. Most of the search power reported in [17, 18] comes from such small S1 signals. Meanwhile, the power law nature of the noise coupled with an event rate of e.g., 5 Hz means that implementing a post-event time-trigger hold-off to reduce the photon rate is at odds with the necessity of maximizing search live time [4].

A fundamental question has remained: *what is the origin of the delayed photon noise?* We have investigated this issue with a 3 cm  $\varnothing$  cylindrical testbed at LBL and conclude that the majority of it is due to fluorescence of quartz<sup>1</sup> photosensor windows, following exposure to UV photons from xenon scintillation.

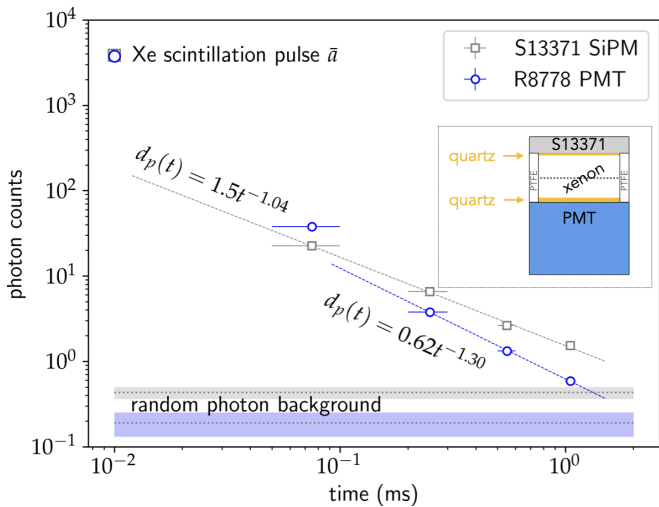


FIG. 2. Measurements of the delayed photon noise count rate per 0.1 ms, following a pulse  $\bar{a}$  of UV photons from xenon scintillation. The experimental configuration is indicated inset.

We initially studied the delayed photon noise with the testbed operated as a TPC i.e., with S1 and S2 pulses [24], in the style of the dark matter search experiments [17, 18]. We subsequently realized that a similar magnitude and time profile of delayed photon noise was also observed following the primary scintillation pulse (S1). The present work is therefore restricted to this simpler case using only S1 as a progenitor pulse, with no applied electric field and no S2 pulse.

To accurately count  $\mathcal{O}(10)$  ns wide delayed single photons over a period of milliseconds following each progenitor

pulse, we employed a “cascade trigger”: the initial 100  $\mu$ s trigger window was automatically followed by three additional 100  $\mu$ s windows, delayed by several hundred microseconds each. This allowed us to methodically sample the photons at later times, without loss of fidelity and within the capabilities of the data acquisition system. The trigger time was set at 10  $\mu$ s in the progenitor pulse window, which allowed an additional data point to be acquired from the last 50  $\mu$ s of the trigger window.

A 2D schematic of the cylindrical experimental configuration is shown in Fig. 2 (inset), indicating the single Hamamatsu R8778 PMT<sup>2</sup> and the array of four, four-channel Hamamatsu S13371 silicon photomultipliers (SiPM) viewing the active region filled with liquid xenon. The four corner channels were not read out, so signals from this array consisted of twelve sensors. Walls were constructed of PTFE, with several 1 mm  $\varnothing$  radial holes (not shown) allowing xenon to flow into and out of the active region. A single high-transparency mesh grid bifurcated the region, and a  $^{210}\text{Po}$  alpha particle source plated in the center of the mesh caused xenon scintillation pulses at a rate of about 10 Hz. We verified by transitory removal that the mesh is unrelated to the presence of delayed photon noise. The testbed was maintained at a constant temperature  $T = (-99 \pm 1)$  °C, with a calibration uncertainty of about 1 C.

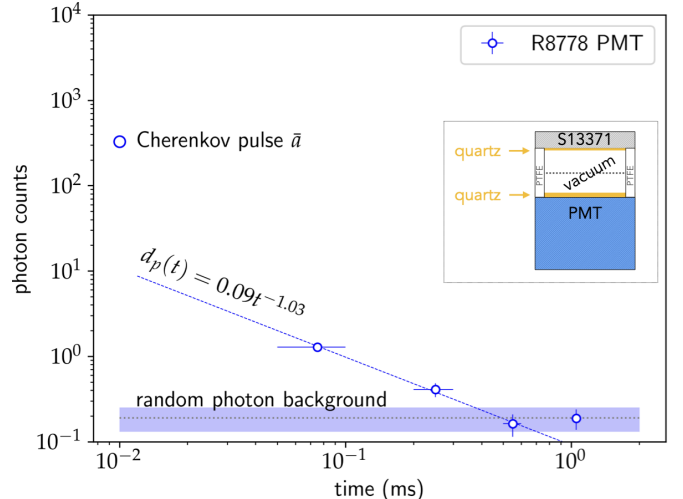


FIG. 3. Measurements of the delayed photon noise count rate per 0.1 ms, following a pulse  $\bar{a}$  of Cherenkov photons. The experimental configuration is indicated inset.

The average response of many such measurements is shown in Fig. 2. Delayed photon counts are normalized to 100  $\mu$ s bin width, so the delayed photon rate in Hz is a factor  $\times 10^4$  larger. We observe that for PMT signals greater than a few hundred photons, PMT after-pulsing [25] systematically increases the photon counts in

<sup>1</sup> Optical grade  $\text{SiO}_2$  is often referred to interchangeably in technical literature as fused silica, synthetic silica, or quartz.

<sup>2</sup> Previously deployed in the LUX experiment [12].

the  $50 - 100 \mu\text{s}$  bin, so this data point is excluded from the fit.

In order to test the hypothesis that fluorescence of the quartz window causes delayed photons, we first made the same series of measurements with vacuum in the active region instead of liquid xenon. The temperature was again maintained at  $T = (-99 \pm 1)^\circ\text{C}$ . Gaseous xenon was used to thermalize the entire testbed for a period of several days, after which the xenon was removed and the active region was evacuated to a pressure of  $1 \times 10^{-6}$  mBar. This low pressure was maintained by constant vacuum pumping during the measurement. Cherenkov photons from radioactive decays in or on the surface of the PMT window were used as a source of UV photon pulses. The results are shown in Fig. 3. We estimate the PMT should detect approximately 300 Cherenkov photons from a 1 MeV beta in its 2 mm thick window. The Cherenkov signal decays faster than xenon scintillation, and has a continuous spectrum that rises sharply toward shorter wavelengths [26]. The PMT response cuts off at  $\lambda = 160 \text{ nm}$ . Due to the small average progenitor pulse  $\bar{a}$ , the response of the S13371 SiPM sensors was barely above the background photon count rate and is not shown. Measured values of  $\alpha$  are within a factor  $\times 2$ . These measurements confirm that quartz is a source of fluorescence with a magnitude and time profile similar to the observed  $d_p(t)$  in liquid xenon TPCs.

In order to conclusively identify quartz fluorescence as the primary source of delayed photons following xenon scintillation, we adapted the experimental configuration as shown in Fig. 4: the active region was divided with a piece of aluminum, in order to optically isolate the upper and lower halves. The PMT was replaced with an array of four, windowless Hamamatsu S13370 SiPM. Of the four sensors, two exhibited excessive leakage current and were left unbiased. Of the remaining two, one showed lower dark counts and so we report data from that single sensor. A single channel of the twelve S13371 sensors was used as a comparison in this case. The active region was completely filled with liquid xenon, and a flow-through  $^{220}\text{Rn}$  alpha particle source was used to provide xenon scintillation pulses. Because of the optical isolation, triggering on a pulse from the S13371 sensor was accompanied by random (mostly zero) photon counts in the S13370 sensor, and vice versa.

The two data sets were acquired separately and are shown together in Fig. 4. The random photon background rate in the single S13371 sensor is an order of magnitude smaller than that of the S13370 and is not shown. In the absence of a window, the fluorescence is reduced by a factor  $\times 15$  in the  $50 - 100 \mu\text{s}$  bin. A smaller, residual component to the delayed photon noise appears to follow an exponential with a time constant  $\tau = 1 \text{ ms}$ . This could be due to fluorescence of the silicon sensor, the ceramic package of the sensor, the PTFE or its impurities, impurities within the xenon or perhaps the xenon

itself. We previously explored varying states of degraded xenon purity and saw no significant difference in the measured  $d_p(t)$ . We also previously explored replacing the PTFE with aluminum, and found no significant reduction in  $d_p(t)$ . However, those investigations were made with S13371 sensors, so the quartz fluorescence may have obscured subtler effects. PTFE fluorescence has long been suspected as a source of  $d_p(t)$  [11, 12], although dedicated measurements found no such effect [27].

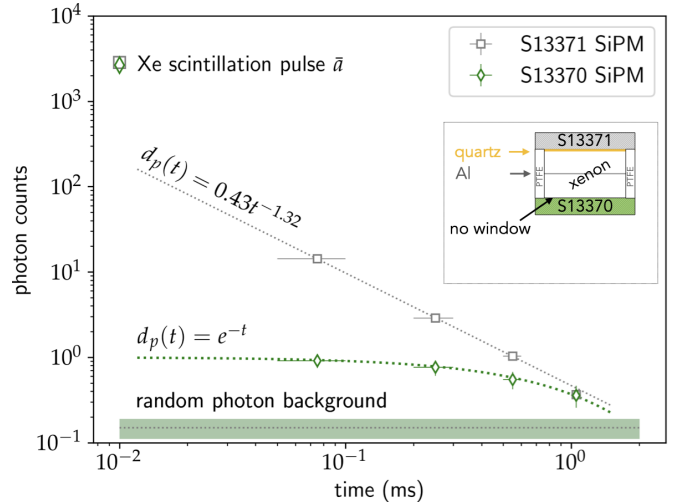


FIG. 4. Delayed photon noise measured in two symmetric, optically isolated regions, one with a quartz window and one without.

We have identified the dominant component of delayed photon noise in liquid xenon particle detectors as fluorescence of quartz windows in the photosensors. More generally, this effect could be present in any experiment which seeks to measure small UV scintillation signals interspersed with a background of larger signals. The cut-off wavelength for fluorescence is at least  $\lambda_c > 350 \text{ nm}$  [28]. Photoluminescence of glass due to impurities is well-known [29], and power law fluorescence is generally attributed to charge-trapping on point defects [30]. The fluorescence is often referred to as phosphorescence when the lifetime extends into the ms regime [29] (as in the present case). A very high purity quartz called VIOSIL manufactured by Shin-Etsu [28] appears to have no measured fluorescence, in contrast to fused quartz. The windows used in the Hamamatsu sensors are specified as “synthetic silica.” We are not aware of any other measurements of the time dependence of quartz glass fluorescence on timescales  $\lesssim 1 \text{ second}$ . Early work [31] found a power law decay on a scale of minutes following exposure to intense source of ultraviolet radiation. More recent studies of electron-induced fluorescence in PMT windows [32, 33] was motivated by excessive dark counts observed in PMTs on space flight experiments, and found multiple exponential components to the fluorescence on timescales  $\gtrsim 1 \text{ minute}$ .

A few aspects of the data deserve additional comment: (a) In Fig. 2 the two sensors record different power law exponents in  $d_p(t)$ . The S13371 retains considerable quantum efficiency for IR photons with  $\lambda > 900$  nm, whereas the PMT response is effectively zero by  $\lambda \sim 700$  nm. If lower-energy fluorescent photons persist more effectively at later times, this could explain the slower decrease in  $d_p(t)$  as measured by the S13371. (b) The same S13371 sensor records different power law exponents in the two experimental configurations. In the case of Fig. 2, two different quartz samples are fluorescing (PMT window and SiPM window) whereas in the case of Fig. 4, only the SiPM window is fluorescing. It seems likely that the different quartz samples exhibit slightly different fluorescent responses. (c) We observe that the power law exponent depends mildly on the size of the progenitor pulse, varying in the range  $0.8 \lesssim k \lesssim 1.5$  and eventually reaching a plateau for sufficiently large signals. This is likely related to the total pulse rate, which affects the background photon count rate. We emphasize that while these observations are certainly worthy of further characterization, the key point of the present work is simply to identify the cause of and eliminate  $d_p(t)$  (viz. Fig. 4).

This investigation comes too late to help the current generation of leading dark matter search instruments, but it could be critical to the design choices of future experiments, such as the proposed XLZD experiment [34]. For example, if PMTs are to continue to be used as photosensors, new R&D should focus on minimizing the UV-induced fluorescence from window materials such as quartz, MgF, and others. Such improvements could potentially lead to a delayed noise rate and profile similar to the exponential curve optimistically shown in Fig. 1. This would drastically alter the ratio of signal to background in experiments such as [17, 18], and improve discovery potential. Alternatively, silicon photomultipliers do not strictly need a window at all, other than to protect the sensor face. However, silicon-based sensors have other challenges, such as higher dark count rates even for optimized devices [35] as well as external crosstalk [23].

We thank Shingo Kazama, Tom Shutt and Jingke Xu for interesting discussions and comments.

---

\* [pfsorensen@lbl.gov](mailto:pfsorensen@lbl.gov)

- [1] N. Aghanim *et al.* (Planck), Planck 2018 results. VI. Cosmological parameters, *Astron. Astrophys.* **641**, A6 (2020), [Erratum: *Astron. Astrophys.* 652, C4 (2021)], arXiv:1807.06209 [astro-ph.CO].
- [2] Y. Sofue and V. Rubin, Rotation curves of spiral galaxies, *Ann. Rev. Astron. Astrophys.* **39**, 137 (2001), arXiv:astro-ph/0010594.
- [3] M. Schumann, Direct Detection of WIMP Dark Matter: Concepts and Status, *J. Phys. G* **46**, 103003 (2019), arXiv:1903.03026 [astro-ph.CO].
- [4] J. Aalbers *et al.* (LZ), Dark Matter Search Results from 4.2 Tonne-Years of Exposure of the LUX-ZEPLIN (LZ) Experiment, (2024), arXiv:2410.17036 [hep-ex].
- [5] E. Aprile *et al.* (XENON), WIMP Dark Matter Search using a 3.1 tonne  $\times$  year Exposure of the XENONnT Experiment, (2025), arXiv:2502.18005 [hep-ex].
- [6] Y. Meng *et al.* (PandaX-4T), Dark Matter Search Results from the PandaX-4T Commissioning Run, *Phys. Rev. Lett.* **127**, 261802 (2021), arXiv:2107.13438 [hep-ex].
- [7] L. Baudis, Dual-phase xenon time projection chambers for rare-event searches, *Phil. Trans. Roy. Soc. Lond. A* **382**, 20230083 (2023), arXiv:2311.05320 [physics.ins-det].
- [8] K. Abe, K. Hiraide, K. Ichimura, Y. Kishimoto, K. Kobayashi, M. Kobayashi, S. Moriyama, M. Nakahata, H. Ogawa, K. Sato, H. Sekiya, T. Suzuki, O. Takachio, A. Takeda, S. Tasaka, M. Yamashita, B. Yang, N. Kim, Y. Kim, Y. Itow, K. Kanzawa, K. Masuda, K. Martens, Y. Suzuki, B. D. Xu, K. Miuchi, N. Oka, Y. Takeuchi, Y. Kim, K. Lee, M. Lee, Y. Fukuda, M. Miyasaka, K. Nishijima, K. Fushimi, G. Kanzaki, and S. Nakamura, A measurement of the scintillation decay time constant of nuclear recoils in liquid xenon with the xmass-i detector, *Journal of Instrumentation* **13** (12), P12032.
- [9] J. Angle *et al.* (XENON10), A search for light dark matter in XENON10 data, *Phys. Rev. Lett.* **107**, 051301 (2011), [Erratum: *Phys. Rev. Lett.* 110, 249901 (2013)], arXiv:1104.3088 [astro-ph.CO].
- [10] R. Essig, A. Manalaysay, J. Mardon, P. Sorensen, and T. Volansky, First Direct Detection Limits on sub-GeV Dark Matter from XENON10, *Phys. Rev. Lett.* **109**, 021301 (2012), arXiv:1206.2644 [astro-ph.CO].
- [11] P. Sorensen and K. Kamdin, Two distinct components of the delayed single electron noise in liquid xenon emission detectors, *JINST* **13** (02), P02032, arXiv:1711.07025 [physics.ins-det].
- [12] D. S. Akerib *et al.* (LUX), Investigation of background electron emission in the LUX detector, *Phys. Rev. D* **102**, 092004 (2020), arXiv:2004.07791 [physics.ins-det].
- [13] T.J. Anderson, The LZ dark matter WIMP search and treatment of fundamental signals, Stanford University (2023).
- [14] D. E. Kaplan, M. A. Luty, and K. M. Zurek, Asymmetric Dark Matter, *Phys. Rev. D* **79**, 115016 (2009), arXiv:0901.4117 [hep-ph].
- [15] D. E. López-Fogliani, A. D. Perez, and R. Ruiz de Austri, Dark matter candidates in the nmssm with rh neutrino superfields, *Journal of Cosmology and Astroparticle Physics* **2021** (04), 067.
- [16] K. Wang, J. Zhu, and Q. Jie, Higgsino asymmetry and direct-detection constraints of light dark matter in the nmssm with non-universal higgs masses \*, *Chinese Physics C* **45**, 041003 (2021).
- [17] W. Ma *et al.* (PandaX), Search for Solar B8 Neutrinos in the PandaX-4T Experiment Using Neutrino-Nucleus Coherent Scattering, *Phys. Rev. Lett.* **130**, 021802 (2023), arXiv:2207.04883 [hep-ex].
- [18] E. Aprile *et al.* (XENON), First Indication of Solar B8 Neutrinos via Coherent Elastic Neutrino-Nucleus Scattering with XENONnT, *Phys. Rev. Lett.* **133**, 191002 (2024), arXiv:2408.02877 [nucl-ex].
- [19] E. Aprile *et al.* (XENON), The XENONnT dark matter experiment, *Eur. Phys. J. C* **84**, 784 (2024),

arXiv:2402.10446 [physics.ins-det].

[20] B. J. Mount *et al.*, LUX-ZEPLIN (LZ) Technical Design Report, (2017), arXiv:1703.09144 [physics.ins-det].

[21] J. Aalbers *et al.* (LZ), First Dark Matter Search Results from the LUX-ZEPLIN (LZ) Experiment, *Phys. Rev. Lett.* **131**, 041002 (2023), arXiv:2207.03764 [hep-ex].

[22] L. Baudis, A. Behrens, A. Ferella, A. Kish, T. Marro-dan Undagoitia, D. Mayani, and M. Schumann, Performance of the Hamamatsu R11410 Photomultiplier Tube in cryogenic Xenon Environments, *JINST* **8**, P04026, arXiv:1303.0226 [astro-ph.IM].

[23] R. Gibbons, H. Chen, S. J. Haselschwardt, Q. Xia, and P. Sorensen, Why would you put a flashlight in a dark matter detector?, *JINST* **19** (01), P01013, arXiv:2309.07913 [physics.ins-det].

[24] R. Gibbons and P. Sorensen, Towards discovery of hidden sector dark matter with liquid xenon TPCs, 15th International Workshop on the Identification of Dark Matter, L'Aquila, IT (2024).

[25] C. H. Faham, *Prototype, Surface Commissioning and Photomultiplier Tube Characterization for the Large Underground Xenon (LUX) Direct Dark Matter Search Experiment*, Ph.D. thesis, Brown U. (2014).

[26] S. Navas *et al.* (Particle Data Group), Review of particle physics, *Phys. Rev. D* **110**, 030001 (2024).

[27] G. R. Araujo, T. Pollmann, and A. Ulrich, Photoluminescence response of acrylic (pmma) and polytetrafluoroethylene (ptfe) to ultraviolet light: Limits on low-intensity photoluminescence in support materials of rare-event search experiments, *The European Physical Journal C* **79**, 10.1140/epjc/s10052-019-7152-2 (2019).

[28] Shin-etsu Chemical Co. Ltd., Synthetic Quartz Technical Datasheet, (2023), <https://www.shinetsu.co.jp//wp-content/uploads/2019/05/Synthetic-Quartz-Glass-Substrates.pdf>.

[29] R. Jedamzik, F. Elsmann, A. Engel, U. Petzold, and J. Pleitz, Introducing the quantum efficiency of fluorescence of SCHOTT optical glasses, in *Current Developments in Lens Design and Optical Engineering XVIII*, Vol. 10375, edited by R. B. Johnson, V. N. Mahajan, and S. Thibault, International Society for Optics and Photonics (SPIE, 2017) p. 1037508.

[30] D. J. Huntley, An explanation of the power-law decay of luminescence, *Journal of Physics: Condensed Matter* **18**, 1359 (2006).

[31] W. H. Coop and J. A. Hammond, Phosphorescence of fused quartz and sapphire, *J. Opt. Soc. Am.* **52**, 835 (1962).

[32] W. Viehmann, A. Eubanks, G. Pieper, and J. Bredekamp, Photomultiplier window materials under electron irradiation: fluorescence and phosphorescence, *Applied Optics* **14**, 2104 (1975).

[33] S. N. Osterman, Thermal and time dependence of radiation-induced phosphorescence in UV window materials, in *UV, X-Ray, and Gamma-Ray Space Instrumentation for Astronomy XIV*, Vol. 5898, edited by O. H. W. Siegmund, International Society for Optics and Photonics (SPIE, 2005) p. 58981H.

[34] J. Aalbers *et al.*, A next-generation liquid xenon observatory for dark matter and neutrino physics, *J. Phys. G* **50**, 013001 (2023), arXiv:2203.02309 [physics.ins-det].

[35] S. Sakamoto, T. Hasegawa, Y. Itow, S. Kazama, M. Kobayashi, and M. Yamashita, Development of a low-noise SiPM for the DARWIN experiment, *PoS ICRC2023*, 1435 (2023).